ChemComm

Amphiphile Self-Assembly Dynamics at the Solution-Solid Interface Reveal Asymmetry in Head/Tail Desorption

Journal:	*ChemComm*
Manuscript ID	CC-COM-06-2018-004465.R1
Article Type:	Communication

ChemComm

COMMUNICATION

Amphiphile Self-Assembly Dynamics at the Solution-Solid Interface Reveal Asymmetry in Head/Tail Desorption

Received 00th January 20xx,
Accepted 00th January 20xx

DOI: 10.1039/x0xx00000x

www.rsc.org/

Henry D. Castillo[a]†, John M. Espinosa-Duran[a]†, James R. Dobscha[a], Daniel C. Ashley[a,b], Sibali Debnath[a], Brandon E. Hirsch[a,c], Samantha R. Schrecke[a,d], Mu-Hyun Baik[a,e], Peter J. Ortoleva[a], Krishnan Raghavachari[a], Amar H. Flood[a], Steven L. Tait[a]*

Amphiphilic alkoxybenzonitriles of varying chain length are studied at the solution / graphite interface to analyze dynamics of assembly. Competitive self-assembly between alkoxybenzonitriles and alkanoic acid solvent is shown by scanning tunneling microscopy (STM) to be controlled by concentration and molecular size. Molecular dynamics (MD) simulations reveal key roles of the sub-nanosecond fundamental steps of desorption, adsorption, and on-surface motion. We discovered asymmetry in desorption-adsorption steps. Desorption starting from alkyl chain detachment from the surface is favored due to dynamic occlusion by neighboring chains. Even though the nitrile head has a strong solvent affinity, it more frequently readsorbs following a detachment event.

Molecular self-assembly at interfaces provides a means to develop highly ordered nanomaterials using bottom-up strategies with applications in electronics, photovoltaics, sensors, and separations.[1-3] Bottom-up strategies rely on precise control over geometry and organization of self-assembled structures, which is only possible through a full understanding of the complex interplay of the intermolecular interactions. Since the advent of STM and pioneering work at liquid-solid interfaces,[4, 5] much has been learned about the roles of supramolecular interactions, chemical potential, and other physical parameters on 2D self-assembly.[2, 6-9] While STM allows sub-molecular resolution of assemblies on flat conductive surfaces, it is limited to those 2D structures that are stable for many seconds. The atomic-level subtleties of picosecond to nanosecond motions remain elusive when using microscopic techniques. Thus, a full understanding of the fundamental steps and molecular design rules governing self-assembly require integrated study by experiment, theory, and computation.

MD simulations offer a means to elucidate how atomistic interactions dictate the sub-nanosecond molecular motions leading to molecular organization during self-assembly on the surface and in solution. MD has been used to understand and design biomolecular systems and synthetic polymers,[10-12] as well as synthetic molecular materials .[13-15] Previous works with STM and MD have shown the power of combining these techniques to understand self-assembly at the interface of solution with highly oriented pyrolytic graphite (HOPG). [16, 17]

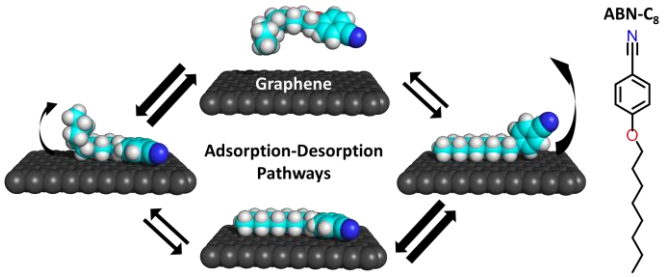

Fig. 1 Possible motions of **ABN-C_8** (inset) on graphite. Top: Fully desorbed. Bottom: fully adsorbed. Left: desorption of alkyl chain. Right: desorption of benzonitrile group.

We present a nanoscale analysis of self-assembly at the solution-solid interface using a synergistic experiment-theory approach. Large scale (>300 nm^2 substrate) atomistic MD simulations for hundreds of ns (2 fs time steps) were conducted in conjunction with STM imaging to study self-assembly of the prototypical molecule alkoxybenzonitrile (**ABN**) on HOPG in octanoic acid (OA) solvent. Alkoxybenzonitriles are easily synthesized and were designed for their amphiphilic character: to examine strong electrostatic (ES) interactions at the polar benzonitrile head group (4.97 D[18]) and van der Waals (vdW)

[a] *Department of Chemistry, Indiana University, 800 E. Kirkwood Avenue, Bloomington, Indiana 47405, USA*
[b] *Current address: Department of Chemistry, North Carolina State University, Raleigh, North Carolina 27695, USA*
[c] *Current address: Division of Molecular Imaging and Photonics, Department of Chemistry, KU Leuven–University of Leuven Celestijnenlaan 200F, 3001 Leuven, Belgium*
[d] *Current address: Department of Chemistry, Texas A&M University, College Station, Texas 77840, USA*
[e] *Current address: Department of Chemistry, Korea Advanced Institute of Science and Technology 291 Daehak-ro, Yuseong-gu Daejeon, 34141, Republic of Korea*
† These authors contributed equally to this work.
* Corresponding author: tait@indiana.edu, Tel.: +1-812-855-1302.
Electronic Supplementary Information (ESI) available: Details of experimental and computational methods. Supplementary data. See DOI: 10.1039/x0xx00000x

interactions of the alkyl chain. The alkyl chain length was modified from 4 to 18 carbons to test the dependence of interdigitation from vdW interactions in alkoxybenzonitrile self-assembly: **ABN-C$_4$**, **ABN-C$_8$**, **ABN-C$_{12}$**, **ABN-C$_{16}$**, and **ABN-C$_{18}$**. Concentration was varied from neat alkoxybenzonitrile (~8 M) to neat solvent to provide insights into the effect of altering the chemical potential of the alkoxybenzonitrile/octanoic acid/HOPG system. Our analysis also reveals that OA is surface active. We present novel observations of the atomistic and sub-nanosecond motions during assembly and make progress toward computer aided design strategies for molecular self-assembly at interfaces (**Fig. 1**).

Surface structures were characterized by STM. The adsorbed structures seen after equilibration at room temperature for various concentrations and chain lengths are summarized in a phase diagram (**Fig. 2a**). STM of high concentrations (≥ 100 mM **ABN-C$_8$**, ≥ 25 mM **ABN-C$_{12}$**, > 10 mM **ABN-C$_{16}$**, ≥ 1.5 mM **ABN-C$_{18}$**) produce a tightly packed alkoxybenzonitrile monolayer with interdigitated alkyl chains (**Fig. 2b**); lower concentrations only show self-assembly of solvent (**Fig. S4**). The phase boundary between OA and alkoxybenzonitrile assemblies depends on alkyl chain length. Assemblies of alkoxybenzonitriles with longer chains are more stable on the surface than those with shorter chains, as expected based on the interaction enthalpy and the entropy of solvent displaced by the adsorbed alkoxybenzonitriles.[19, 20]

The competition between alkoxybenzonitrile vs. OA adsorption is also observed in MD simulations. **ABN-C$_{18}$** (233 mM) and **ABN-C$_{12}$** (286 mM) are found to preferentially adsorb, as seen by STM. However, **ABN-C$_8$** (414 mM) is displaced by OA, even at much higher concentration than for self-assembly in experiment. **ABN-C$_4$** did not adsorb in MD (444 mM) or in experiment (100 uM – 1 M).

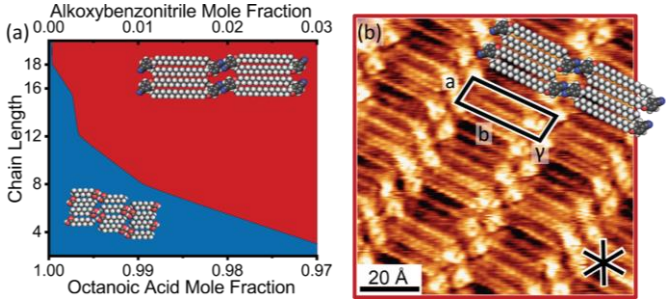

Fig. 2 High resolution STM images and packing models of alkoxybenzonitriles and octanoic acid at the solution/HOPG interface. (a) Phase diagram of alkoxybenzonitriles in octanoic acid as function of alkyl chain length and mole fraction. Blue: octanoic acid self-assembly. Red: alkoxybenzonitrile self-assembly. (b) **ABN-C$_{18}$**. Conditions: 10 mM, I_t= 0.40 nA, V_{sample}= -1.2 V. Refer to **Fig. S4** for STM images of octanoic acid.

The packing density of alkoxybenzonitriles with different alkyl groups scales with the alkyl chain length, indicating full adsorption of the alkyls (**Table S1**). The most notable feature in the STM images is the distinct contrast between two types of rows: the double row of bright round features is attributed to head-to-head packing of aromatic benzonitrile groups[6] and lower contrast rows are assigned to interdigitated alkyl chains. Alkyl chains are aligned with the primary axes of HOPG. A non-ideal alkyl spacing of 4.9 ± 0.3 Å (ideal = 4.4 Å)[21] results in a moiré pattern along lamellar rows (**Fig. 2b**). Alkoxybenzonitrile assembly involves several interactions: (a) C-H•••N-C hydrogen (H-) bonding between aryl hydrogens and cyano nitrogens of the head group, (b) nitrile-nitrile dipolar coupling, and (c) vdW interdigitation of alkyl chains (**Fig. 2b**).

Octanoic acid self-assemblies, by comparison, are characterized by a single row of bright features, attributed to H-bonded carboxylic acids, alternating with lamellar alkyl rows (**Fig. S4**). STM images are consistent with models featuring dimerized carboxylic acid heads and alkyl chains interdigitating to produce lamellar rows. The unit cell is consistent with the size of the octanoic acid dimers and is independent of ABN chain length. Dodecanoic acid was also tested as solvent and adsorbs in the same structures as OA but with wider rows (**Fig. S5**).

MD simulations (1800 nm^3, 2 700 molecules, 120 000 atoms) were undertaken to investigate (1) dynamics of self-assembly starting from an initially disordered state and (2) stability of 2D assemblies starting from the experimentally determined packing structure. Simulations were performed with a constant number of atoms (fixed concentration), volume, and temperature (NVT ensemble).

Simulations starting from an initially ordered state still show interdigitated packing after hundreds of nanoseconds (**Fig. 3a** and **3b**) with unit cells that match experiment to within one standard deviation (**Table S1**). Starting from an ordered state, 22% of **ABN-C$_8$** molecules desorb (**Fig. 3c**), while **ABN-C$_4$** retains an ordered interdigitated structure at 444 mM despite ca. 30% desorption (**Fig. 3c** and **Fig. S6d**). Both **ABN-C$_{12}$** and **ABN-C$_{18}$** also retain the ordered structure, but with almost no desorption. On areas of HOPG not filled with alkoxybenzonitriles, OA assembles as carboxylic acid dimers in an *anti*-parallel fashion producing lamellae (**Fig. 3**), matching solvent structures observed at low alkoxybenzonitrile concentrations (**Fig. S4**).

Of the simulations starting from the disordered state, only **ABN-C$_{18}$** and **ABN-C$_{12}$** yield interdigitated ABN domains (**Fig. 3d** and **Fig. S6f**); initially disordered simulations of **ABN-C$_8$** and **ABN-C$_4$** exhibit desorption and replacement with octanoic acid (**Fig. 3e**, **3f** and **Fig. S6h**). Increased desorption and on-surface lateral movement with shorter alkyl chain length point to the importance of vdW contacts in stabilizing ABN layers.

MD simulations reveal that assembly relies more on vdW interactions between alkyls than H-bonding between benzonitrile dimers. With few exceptions (**ABN-C$_8$** and **ABN-C$_4$** simulations starting from disordered initial states) an *anti*-parallel orientation of alkoxybenzonitriles is always adopted in ordered domains (**Fig. 3** and **Fig. S6**), consistent with STM. Although the *anti*-parallel orientation allows for CH•••NC H-bonding between head groups, alkoxybenzonitriles were observed in MD to shift along the direction of the alkyl chains, disrupting this H-bonding, which is not consistent with the ordered domains in STM images. The dynamics hint that vdW interactions are more influential in the early stages of domain formation in MD. The non-directionality of vdW interactions allows movement of molecules without breaking interactions. That is, the vdW interdigitation offers some structural flexibility

along the direction parallel to the alkyl axis, though this is not favourable for the H-bonding.

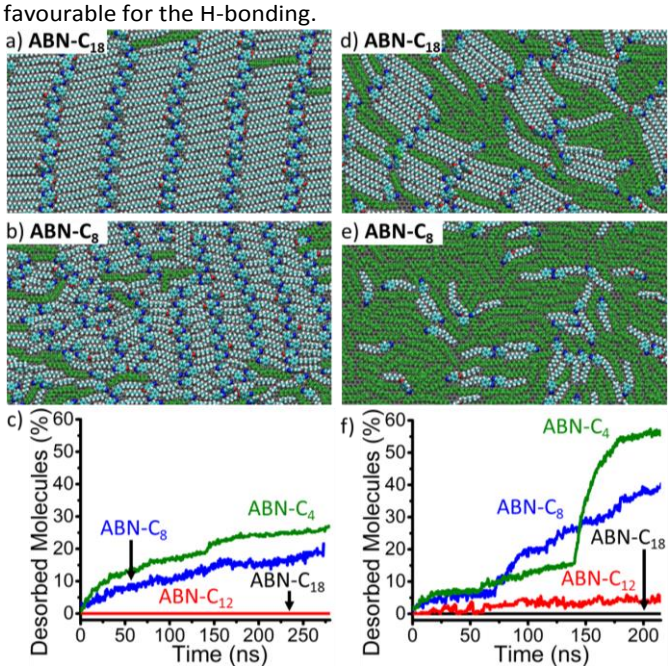

Fig. 3 (a-b) MD simulations of alkoxybenzonitriles in OA (adsorbed OA in green) on HOPG from initially ordered alkoxybenzonitrile state with varying chain length at 280 ns. (d-e) MD simulations from initially disordered alkoxybenzonitrile state with varying chain length at 215 ns. Desorbed alkoxybenzonitrile and octanoic acid molecules have been omitted for clarity. (c and f) Percentage of desorbed alkoxybenzonitriles as a function of time based on analysis of molecular dynamics simulations starting from initially (c) ordered and (f) disordered states. Note that zero desorption is observed for **ABN-C_{18}** for both initial states and **ABN-C_{12}** for the ordered initial states. For images of all alkoxybenzonitrile MD simulations, see **Fig. S6**.

MD simulations that led to alkoxybenzonitrile domains show that alkoxybenzonitriles align with the primary axis of graphite (**Fig. S8**), consistent with experimental results. ABN alkyl chains in MD simulations pack at the most stable density (4.4 Å),[21] which contradicts the observation of the moiré pattern in STM (4.9 Å, **Fig. 2b**). This indicates that the HOPG lattice acts to template the 2D orientation of these organic molecules.

The expected CH•••NC distance (weak H-bond) is 2.75 Å.[22] MD simulations show bond distances clustered near this value, but with a significant spread to even longer H-N lengths (**Fig. 4**, **Fig. S9c**, and **Table S2**). The ideal alignment angle for a single CH•••NC bond is 180°,[22] but the ideal CH•••NC bond angle for a benzonitrile dimer with two CH•••NC bonds is 120° (**Fig. 4** inset), which is consistent with MD simulations (**Fig. 4**, **Fig. S9b**, and **Table S2**). The long CH•••NC distance is consistent with the relatively weak character of this non-traditional hydrogen bond.[22] It seems that assembly is primarily directed by the alkyl interdigitation, with the head group sterics and nitrile H-bonding being secondary interactions in the ordering hierarchy.

Although the CH•••NC bond angles and distances did not change during progression of the simulations from the initially ordered state, we observed a change in angle between the row direction and molecule axis; the final result of each simulation does not match corresponding experimental results (69° vs. 84°). This angle change occurs within the first 60 ns for each of the molecules studied. We considered that this discrepancy might be due to an imbalance in vdW vs. electrostatic interaction strengths in the simulation, but a systematic variation of both of those did not significantly improve the structural match (specifically, the row to molecule axis angle) between experiment and simulation.

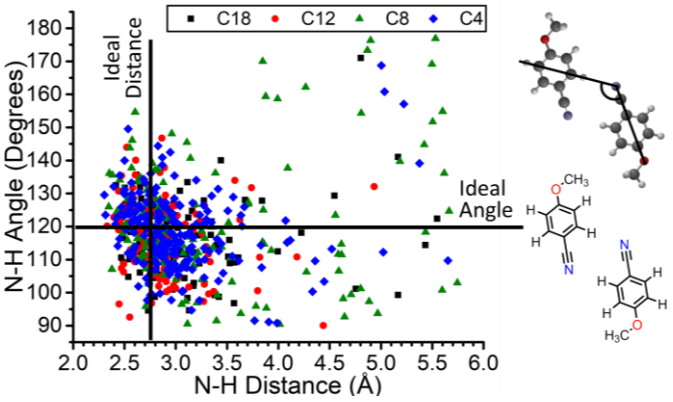

Fig. 4 H-bond angle vs. distance between nitrile nitrogen and aryl hydrogen of paired alkoxybenzonitriles. Plotted alkoxybenzonitriles are the final state of MD simulations from ordered initial states. Right: Benzonitrile model with angle being measured. n=98 **ABN-C_{18}**, n=160 **ABN-C_{12}**, n=152 **ABN-C_8**, n=223 **ABN-C_4**. Measurements taken at 368 ns (**ABN-C_{18}**), 285 ns (**ABN-C_{12}**), 354 ns (**ABN-C_8**), 326 ns (**ABN-C_4**).

We examined the MD simulation results for insight into the fundamental steps of partial detachment, molecular desorption, re-adsorption, and on-surface diffusion that are essential steps in surface self-assembly. Partial detachment of alkoxybenzonitriles is initiated at either end of the molecule, but most often occurs at the benzonitrile head (**Fig. S10a**). As a portion of the molecule detaches from the surface, the free surface area is immediately taken (within several ps) by neighbouring adsorbed molecules. With no open surface available for re-adsorption, molecules may be trapped in a partially desorbed state for over 100 ns until an open area becomes available and re-adsorption becomes possible.

Full desorption of the entire alkoxybenzonitrile occurs by initial partial detachment, followed by peeling off the surface and inhibition of re-adsorption by neighbouring molecules (**Figs. 5a-b**). The timescale of full desorption varies from several ps to hundreds of ns. Unlike partial desorption, full desorption is more often initiated from the alkyl chain than the benzonitrile head (**Fig. S10b**). This is surprising as the benzonitrile should have a greater affinity for the OA solution. The alkyl flexibility contributes to more frequent desorption. As an alkyl chain begins to peel away from the surface, neighbouring molecules fill in the open surface. When this happens, the detached alkyl is prevented from re-adsorbing and further desorption is possible. Unlike the stepwise detachment of flexible alkyls, the rigid benzonitrile detaches completely and re-adsorbs back to its original π-stacked conformation, but usually via edge-on perpendicular interactions with the surface (**Fig. 5c**). The open surface area created by a detached head is wider than an alkyl. Neighbouring adsorbed heads are constrained in their motion by their attachment to the interdigitated alkyls. C–O bond rotations of the detached head groups allow initial re-adsorption in a perpendicular conformation, then the head rotates to a flat-lying orientation.

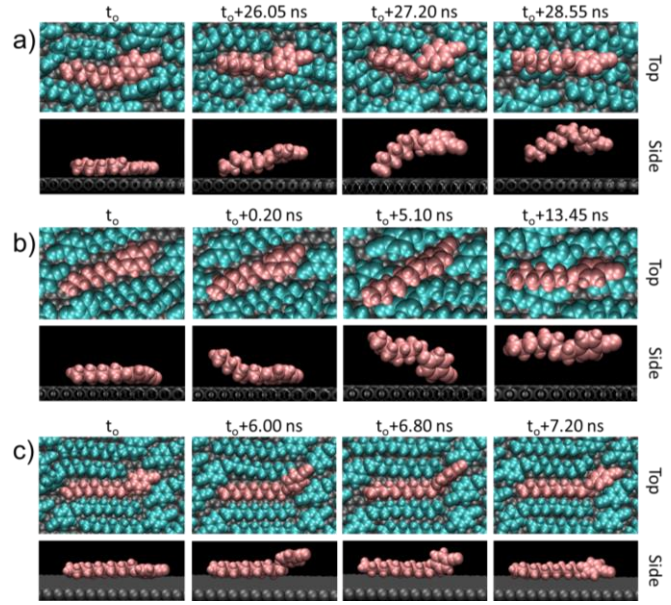

Fig. 5 (a and b) Top down and side view snapshots showing desorption of **ABN-C_8** (pink) starting from the head (a) and chain (b). From left to right, the alkoxybenzonitrile is fully adsorbed (left), partial desorption occurs of either (a) the benzonitrile group or (b) the alkyl chain (center), and desorption (right). (c) Partial desorption and reabsorption of benzonitrile head of **ABN-C_{12}** (pink). From left to right, benzonitrile head is desorbed (left), interacts with the surface in a perpendicular orientation (center), and adsorbs in the ideal parallel orientation with the surface (right).

Adsorption of alkoxybenzonitriles from bulk solution has four stages (**Fig. S11**). First, the benzonitrile head initiates adsorption onto the molecular monolayer through non-specific interactions and accommodates itself in a flat-lying configuration. Next, the alkyl chain follows, CH_2-by-CH_2, onto the existing monolayer. These first two steps occur within 1 ns. Third, the alkoxybenzonitrile diffuses on the monolayer until an open area of HOPG is available. This process may take tens of ns. Fourth, the re-adsorbing alkoxybenzonitrile diffuses into the open graphite area. Either the benzonitrile head or alkyl chain enters first. Depending on the size of the open area and diffusion of adjacent molecules, full adsorption may require several ps to tens of ns. All these details show events that occur over small length and time scales and reveal early stages of assembly where diffusion of molecules from solution to the surface is governed by non-specific vdW interactions.

Atomistic analysis reveals key details of fundamental self-assembly processes. The amphiphilic alkoxybenzonitrile design allows direct comparison of the adsorption/desorption behaviour of aliphatic chains versus polar aromatic head groups. Interestingly, a significant asymmetry in the adsorption/desorption steps is observed due to the differences in the fundamental steps available to these functional groups. MD simulations corroborate the structures derived from sub-molecular resolution STM experiments, thus an interactive experiment-theory feedback benefits both aspects of the study. Atomistic MD simulations give crucial ns resolution of self-assembly not accessible by experiment; extension of these simulations to ms timescales, needed to simulate the entire self-assembly process, will require future advances in multiscale simulation[23] or hybrid Monte Carlo / MD methods.[24, 25]

This work was supported by the National Science Foundation (NSF), Designing Materials to Revolutionize and Engineer the Future program (DMR-1533988). MD calculations were conducted on Indiana University's Big Red II supercomputer supported in part by Lilly Endowment, Inc., Indiana University's Pervasive Technology Institute, and by the Indiana METACyt Initiative. JMED acknowledges support from the Colombian Administrative Department of Science, Technology and Innovation. SRS was supported by the IU Chemistry NSF REU program (CHE-1460720).

Conflicts of interest

There are no conflicts of interest to declare.

Notes and references

1. T. Aida, E. W. Meijer and S. I. Stupp, *Science*, 2012, **335**, 813-817.
2. K. S. Mali, N. Pearce, S. De Feyter and N. R. Champness, *Chem. Soc. Rev.*, 2017, **46**, 2520-2542.
3. L. Sosa-Vargas, E. Kim and A.-J. Attias, *Mater. Horiz.*, 2017, **4**, 570-583.
4. G. Binnig, H. Rohrer, C. Gerber and E. Weibel, *Phys. Rev. Lett.*, 1982, **49**, 57-61.
5. J. P. Rabe and S. Buchholz, *Science*, 1991, **253**, 424-427.
6. B. E. Hirsch, K. P. McDonald, B. Qiao, A. H. Flood and S. L. Tait, *ACS Nano* 2014, **8**, 10858-10869.
7. S. Lee, B. E. Hirsch, Y. Liu, J. R. Dobscha, D. W. Burke, S. L. Tait and A. H. Flood, *Chem. Eur. J.*, 2016, **22**, 560-569.
8. B. E. Hirsch, K. P. McDonald, A. H. Flood and S. L. Tait, *J. Chem. Phys.*, 2015, **142**, 101914.
9. B. E. Hirsch, K. P. McDonald, S. L. Tait and A. H. Flood, *Faraday Discussions*, 2017, **204**, 159-172.
10. M. C. Childers and V. Daggett, *Mol. Syst. Des. Eng.*, 2017, **2**, 9-33.
11. M. De Vivo, M. Masetti, G. Bottegoni and A. Cavalli, *J. Med. Chem.*, 2016, **59**, 4035-4061.
12. S. C. Glotzer and W. Paul, *Annu. Rev. Mater. Res.*, 2002, **32**, 401-436.
13. A. Minoia, I. Destoop, E. Ghijsens, S. De Feyter, K. Tahara, Y. Tobe and R. Lazzaroni, *RSC Advances*, 2015, **5**, 6642-6646.
14. N. Li, H. Jang, M. Yuan, W. Li, X. Yun, J. Lee, Q. Du, R. Nussinov, J. Hou, R. Lal and F. Zhang, *Langmuir*, 2017, **33**, 6647-6656.
15. Y. Liu, A. Singharoy, C. G. Mayne, A. Sengupta, K. Raghavachari, K. Schulten and A. H. Flood, *J. Am. Chem. Soc.*, 2016, **138**, 4843-4851.
16. J. Saiz-Poseu, I. Alcon, R. Alibes, F. Busque, J. Faraudo and D. Ruiz-Molina, *CrystEngComm*, 2012, **14**, 264-271.
17. C.-A. Palma, A. Ciesielski, M. A. Öner, G. Schaeffer, J.-M. Lehn, J. V. Barth and P. Samorì, *Chem. Commun.*, 2015, **51**, 17297-17300.
18. H. Fujiwara, T. Takagi, Y. Yamazaki and Y. Sasaki, *J. Chem. Soc., Faraday Trans.*, 1982, **78**, 347-356.
19. J. F. Dienstmaier, K. Mahata, H. Walch, W. M. Heckl, M. Schmittel and M. Lackinger, *Langmuir*, 2010, **26**, 10708-10716.
20. M. O. Blunt, J. Adisoejoso, K. Tahara, K. Katayama, M. Van der Auweraer, Y. Tobe and S. De Feyter, *J. Am. Chem. Soc.*, 2013, **135**, 12068-12075.
21. A. J. Groszek, *Proc. Royal Soc. London A*, 1970, **314**, 473-498.
22. G. R. Desiraju and T. Steiner, *The Weak Hydrogen Bond*, Oxford University Press, Oxford, 1999.
23. A. Abi Mansour and P. J. Ortoleva, *Journal of Chemical Theory and Computation*, 2014, **10**, 518-523.
24. C. Yuan, S. Li, Q. Zou, Y. Ren and X. Yan, *Phys. Chem. Chem. Phys.*, 2017, **19**, 23614-23631.
25. S. A. Deshmukh, L. A. Solomon, G. Kamath, H. C. Fry and S. K. Sankaranarayanan, *Nat. Commun.*, 2016, **7**, 12367.

Table of Contents entry

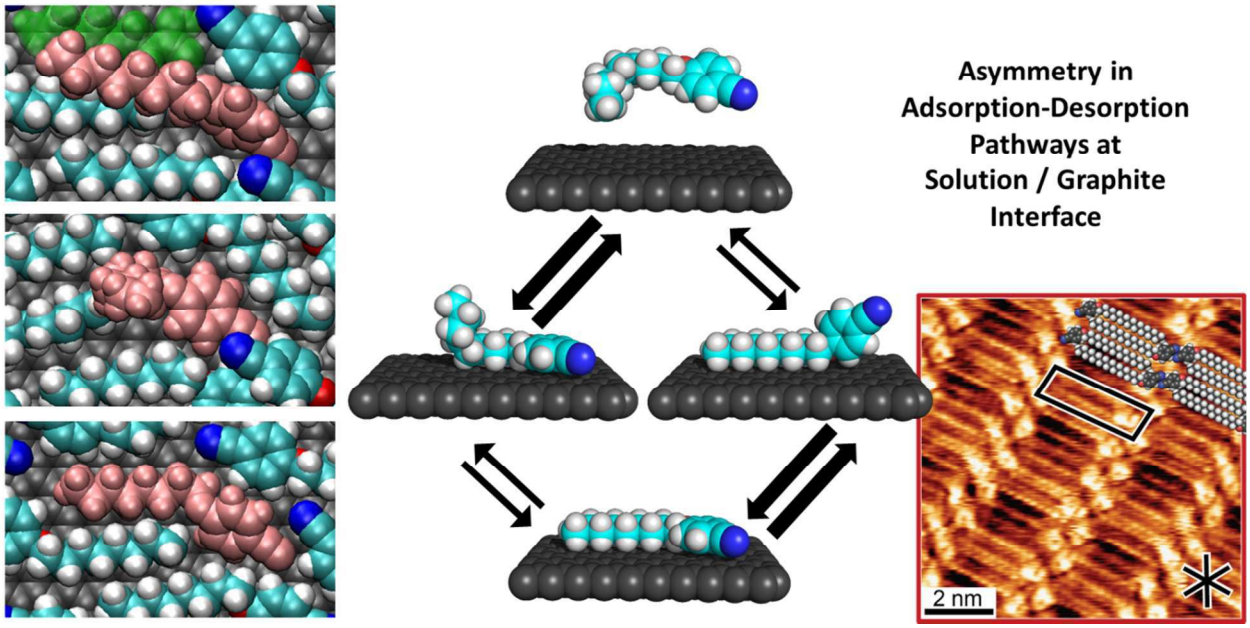

Asymmetric dynamics in fundamental adsorption and desorption steps drive self-assembly at solution / solid interface.